Journal of Biomolecular NMR, **16:** 221–227, 2000.
KLUWER/ESCOM

Transverse relaxation optimised spin-state selective NMR experiments for measurement of residual dipolar couplings

Perttu Permi[a] & Arto Annila[b,*]
[a]*Institute of Biotechnology, NMR Laboratory, P.O. Box 56, 00014 University of Helsinki, Helsinki, Finland;*
[b]*VTT Biotechnology, FIN-02044 VTT, Espoo, Finland*

Received 27 September 1999; Accepted 24 December 1999

Key words: dipolar couplings, SAR by NMR, spin-state-selective filters, TROSY

Abstract

Three transverse relaxation optimised NMR experiments (TROSY) for the measurement of scalar and dipolar couplings suitable for proteins dissolved in aqueous iso- and anisotropic solutions are described. The triple-spin-state-selective experiments yield couplings between $^{1}H^{N}$-$^{13}C^{\alpha}$, ^{15}N-$^{13}C^{\alpha}$, $^{1}H^{N}$-$^{13}C^{\alpha}_{i-1}$, ^{15}N-$^{13}C^{\alpha}_{i-1}$, $^{1}H^{N}$-$^{13}C'_{i-1}$, ^{15}N-$^{13}C'_{i-1}$, and $^{13}C'_{i-1}$-$^{13}C^{\alpha}_{i-1}$ without introducing nonessential spectral crowding compared with an ordinary two-dimensional ^{15}N-^{1}H correlation spectrum and without requiring explicit knowledge of carbon assignments. This set of α/β-*J*-TROSY experiments is most useful for perdeuterated proteins in studies of structure–activity relationships by NMR to observe, in addition to epitopes for ligands, also conformational changes induced by binding of ligands.

Introduction

Destructive relaxation interference of ^{15}N-^{1}H dipole-dipole (DD) and ^{15}N chemical shift anisotropy (CSA) interactions at high magnetic field provides a means for NMR study of macromolecules far larger than was earlier anticipated (Pervushin et al., 1997, 1998a–c; Salzmann et al., 1998, 1999; Yang and Kay, 1999). Transverse relaxation optimised spectroscopy (TROSY) is most amenable to perdeuterated proteins, in which there are only a few routes for amide proton relaxation (Pervushin et al., 1997). Consequently, there are comparatively few interproton distances to be extracted from nuclear Overhauser enhancements for determination of three-dimensional structures. However, directional information contained in residual dipolar couplings is readily available from proteins dissolved into dilute liquid crystals (Bax and Tjandra, 1997; Tjandra and Bax, 1997). Internuclear directions not only supply constraints for the structure determination (Tjandra and Bax, 1997), but provide other biologically significant information, e.g., data relevant to the recognition of protein folds (Annila et al., 1999). Several dipolar couplings measured conveniently from two-dimensional ^{15}N-^{1}H correlation spectra implemented with TROSY, thus superficially resembling a conventional ^{15}N-^{1}H HSQC spectrum, would give insight into conformational changes induced by ligand binding. This approach is analogous to structure–activity relationship (SAR) studies by NMR (Fesik, 1993; Hajduk et al., 1996; Shuker et al., 1997) in which binding epitopes are localised from changes in chemical shifts.

We describe transverse relaxation optimised NMR experiments for the measurement of scalar and dipolar couplings suitable for perdeuterated proteins dissolved in aqueous iso- and anisotropic solutions. These three experiments yield couplings between $^{1}H^{N}$-$^{13}C^{\alpha}$, ^{15}N-$^{13}C^{\alpha}$, $^{1}H^{N}$-$^{13}C^{\alpha}_{i-1}$, ^{15}N-$^{13}C^{\alpha}_{i-1}$, $^{1}H^{N}$-$^{13}C'_{i-1}$, ^{15}N-$^{13}C'_{i-1}$, and $^{13}C'_{i-1}$-$^{13}C^{\alpha}_{i-1}$ without requiring explicit knowledge of carbon assignments (Figure 1). In addition, ^{15}N-^{1}H couplings are available in each of three experiments when using the generalised TROSY-selection.

*To whom correspondence should be addressed. E-mail: Arto.Annila@vtt.fi

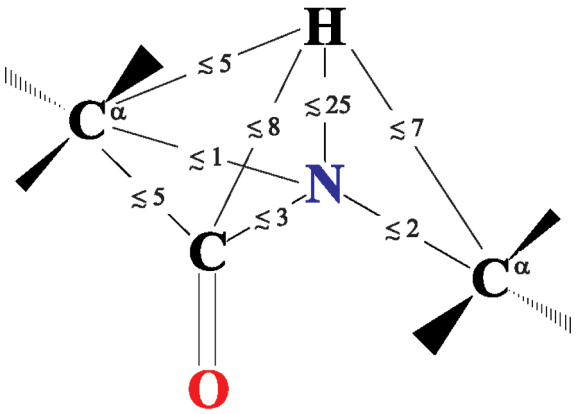

Figure 1. In the plane of the peptide bond there are several couplings that are expected to contain large enough residual dipolar contributions to be measured accurately. The values of various dipolar contributions (in Hz) are indicated relative to a maximal 25 Hz $^{1}H^{N}$-^{15}N dipolar coupling.

Results and discussion

The pulse sequences, referred to here as HN(CO-α/β-NC$^{\alpha}$-*J*)-TROSY, HN(α/β-NC′-*J*)-TROSY (Permi et al., 1999a), and HN(CO-α/β-C′C$^{\alpha}$-*J*)-TROSY, contain common building blocks (Figure 2). Initially, sequential heteronuclear polarisation elements transfer magnetisation from $^{1}H^{N}$ to the target nucleus, i.e., ^{15}N, $^{13}C'_{i-1}$, subject to the couplings of interest. Subsequent spin-state-selective filter elements (Meissner et al., 1997a, b; Andersson et al., 1998a, b; Ottiger et al., 1998; Permi et al., 1999a, b) generate in- and antiphase components which co-evolve with the chemical shift of ^{15}N. Finally, in reverse transfer steps, $^{1}H^{N}$ and ^{15}N spin-states are selected with the sensitivity enhanced TROSY element (Andersson et al., 1998c; Czisch and Boelens, 1998; Meissner et al., 1998a; Pervushin et al., 1998a). The coupling of the passive spin with ^{15}N during the evolution (t_1) and with $^{1}H^{N}$ during the acquisition (t_2) gives rise to splittings on the most slowly relaxing $^{1}H^{N}$-^{15}N cross peak. The couplings can be measured from the multiplet components, separated into two subspectra, with high sensitivity and resolution without the introduction of unnecessary spectral crowding relative to the conventional HSQC (Bodenhausen and Ruben, 1980; Bax et al., 1990).

The HN(CO-α/β-NC$^{\alpha}$-*J*)-TROSY experiment (Figure 2A) enables measurement of $^{1}H^{N}$-$^{13}C^{\alpha}$, ^{15}N-$^{13}C^{\alpha}$, $^{1}H^{N}$-$^{13}C^{\alpha}_{i-1}$, ^{15}N-$^{13}C^{\alpha}_{i-1}$ couplings, which are intrinsically difficult to resolve. In addition to dipolar couplings carrying directional information, the intra- and interresidue ^{15}N-$^{13}C^{\alpha}$ scalar couplings correlate with protein secondary structure (Delaglio et al., 1991). The separation of the intra- and interresidue couplings, which are of comparable strength (Bystrov, 1976; Delaglio et al., 1991), relies on the large and approximately uniform $^{1}J_{C'C^{\alpha}}$ (∼55 Hz) for the creation of either $4H_zN_yC'_z$ or $8H_zN_yC'_zC^{\alpha}_z$ spin coherence before t_1. The undesired dispersive magnetisation component arising from the *J*-mismatch of the filter is purged by the field crusher gradient pulse, in a manner analogous to the pulsed field gradient (PFG) z-filter. During the following ^{15}N chemical shift evolution, which is implemented as a semi-constant time (S-CT) (Grzesiek and Bax, 1993a; Logan et al., 1993) for improved resolution and sensitivity, the in- and antiphase $^{13}C'_{i-1}$-$^{13}C^{\alpha}_{i-1}$ magnetisations couple to ^{15}N simultaneously with the intraresidue $^{13}C^{\alpha}$. Both the intra- and interresidue $^{13}C^{\alpha}$ act as common passive spins during t_1 and t_2, hence a familiar E.COSY pattern (Griesinger et al., 1985, 1986, 1987) emerges. In this way the complex coupling pattern of overlapping ‘doublets of doublets’ is simplified to contain in each of the two subspectra only the in-phase doublets. The selection is then made for the most slowly relaxing $^{1}H^{N}$-^{15}N multiplet component that gives the narrowest lines. The intraresidue $J_{NC^{\alpha}}$ and $J_{H^{N}C^{\alpha}}$ are obtained from the apparent splittings of the in-phase multiplet and, in the case of broad lines, by applying line width-dependent corrections. The interresidue $^{1}H^{N}$-$^{13}C^{\alpha}_{i-1}$ and ^{15}N-$^{13}C^{\alpha}_{i-1}$ couplings are invariably resolved by the spin-state selection. The improvement over the $^{13}C^{\alpha}$-coupled and $^{13}C'$-decoupled TROSY spectrum is indisputable (Figure 3). Good filtering as a function of *J*-mismatch is provided also in the presence of residual dipolar couplings (Permi et al., 1999b). Dipolar contribution to the $^{13}C'$-$^{13}C^{\alpha}$ coupling can be expected in the range from −5 to 5 Hz, when the maximal dipolar contribution to the ^{15}N-^{1}H splitting is 20–25 Hz. In the range of 43–68 Hz, the intensity of the undesired minor component arising from the *J*-mismatch of the filter is at least 30 times smaller compared with the intensity of the principal components.

The HN(α/β-NC′-*J*)-TROSY (Permi et al., 1999a) experiment (Figure 2B) is preferred over the non-filtered $^{13}C'$-coupled IPAP-HSQC experiment (Wang et al., 1998) because the ^{15}N-$^{13}C'$ doublets are separated to two subspectra so as not to increase spectral crowding. The subspectral editing is based on relatively small ^{15}N-$^{13}C'$ coupling, which in the isotropic phase varies from 14 to 16 Hz for the majority of

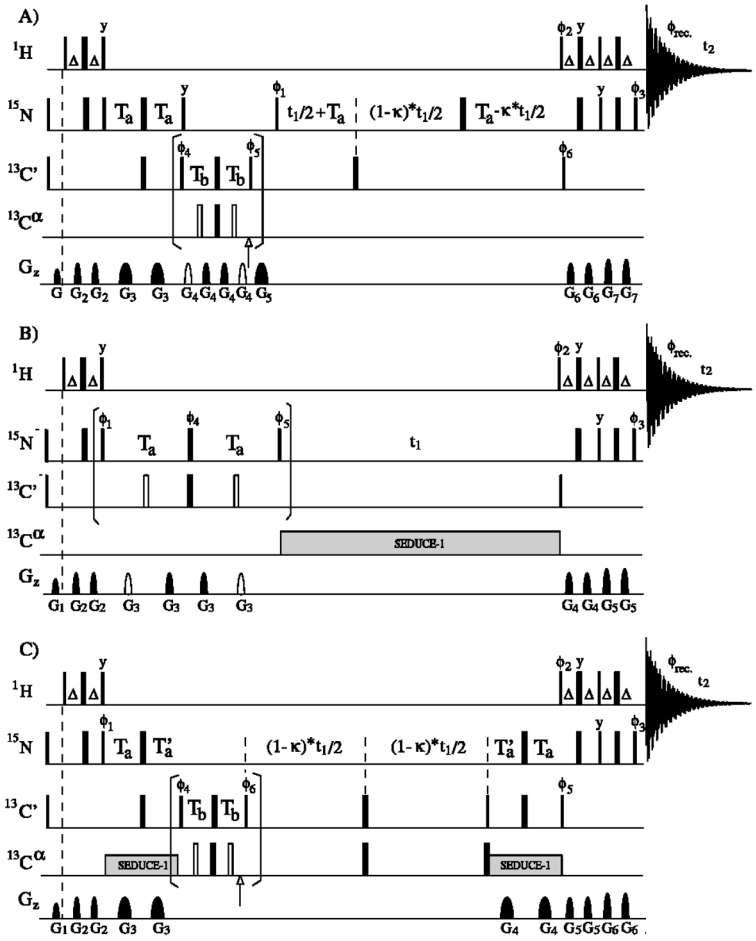

Figure 2. Sensitivity enhanced spin-state selective TROSY pulse sequences for determination of scalar and dipolar couplings from 2D ^{15}N-^{1}H correlation spectra. Narrow (wide) bars correspond to 90° (180°) pulses, with phase x unless otherwise indicated. All ^{13}C′ and (^{13}C$^{\alpha}$) 90° (180°) pulses are applied with a strength of $\Delta/\sqrt{15}$ ($\Delta/\sqrt{3}$), where Δ is the frequency difference between the centers of the ^{13}C′ and ^{13}C$^{\alpha}$ regions. The ^{1}H, ^{15}N, and ^{13}C′ carrier positions are 4.7 (water), 120 (center of ^{15}N spectral region), and 175 ppm (center of ^{13}C′ spectral region), respectively. Two data sets, both for the in- and antiphase spectra, are collected (I): $\phi_2 = y$; $\phi_3 = x$, (II): $\phi_2 = -y$; $\phi_3 = -x$; States-TPPI (Marion et al., 1989) on ϕ_1. The addition and subtraction of (I) and (II), and subsequent addition (subtraction) with appropriate phase correction of resulting intermediate sets yields the spectrum with the most slowly (rapidly) relaxing ^{15}N-^{1}H cross peak. In- and antiphase data are subsequently added and subtracted to separate the multiplet components to two subspectra. (A) Pulse sequence for the determination of the $^{1}J_{\mathrm{NC}^{\alpha}}$ ($^{2}J_{\mathrm{NC}^{\alpha}}$) and $^{2}J_{\mathrm{H^{N}C}^{\alpha}}$ ($^{3}J_{\mathrm{H^{N}C}^{\alpha}}$) couplings by the 2D HN(CO-α/β-NC$^{\alpha}$-*J*)-TROSY experiment. The delays employed are: $\Delta = 1/(4J_{\mathrm{NH}})$; $\mathrm{T_a} = 1/(4J_{\mathrm{NC'}})$; $\mathrm{T_b} = 1/(4J_{\mathrm{C'C}^{\alpha}})$; $0 \le \kappa \le \mathrm{T_a}/t_{1,\mathrm{max}}$. Phase cycling for the in-phase spectrum: ϕ_1 = x, −x; ϕ_4 = 2(x), 2(−x); ϕ_5 = x; ϕ_6 = 4(x), 4(−x); $\phi_{\mathrm{rec.}}$ = x, 2(−x), x; for the antiphase spectrum: $\phi_5 = y$. The arrow indicates the position of the Bloch-Siegert compensation pulse in the antiphase filter. Quadrature detection in the F_1-dimension is obtained by altering the phase of ϕ_1 according to States-TPPI. The resolution in the ^{15}N-dimension is improved by implementing an evolution period for the ^{15}N chemical shift and the ^{15}N-^{13}C$^{\alpha}$ couplings in a semi-constant time manner. The duration of all the pulsed field gradients is 1 ms and strengths are as follows: $G_1 = 4$ G/cm; $G_2 = 5.5$ G/cm; $G_3 = 12.3$ G/cm; $G_4 = 7.2$ G/cm; $G_5 = 16.5$ G/cm; $G_6 = 22$ G/cm; $G_7 = 30.1$ G/cm. (B) Pulse sequence for the determination of $^{1}J_{\mathrm{NC'}}$ in a 2D HN(α/β-NC′-*J*)-TROSY experiment (Permi et al., 1999a). The delays employed are $\Delta = 1/(4J_{\mathrm{NH}})$; $\mathrm{T_a} = 1/(4J_{\mathrm{NC'}})$; phase cycling for the in-phase spectrum: ϕ_1 = y, −y; ϕ_4 = y; ϕ_5 = 2(x), 2(−x); $\phi_{\mathrm{rec.}}$ = 2(x, −x). Phase cycling for the antiphase spectrum: ϕ_1 = x, −x; ϕ_4 = x; ϕ_5 = 2(x), 2(−x); $\phi_{\mathrm{rec.}}$ = 2(x, −x). States-TPPI on ϕ_1. SEDUCE-1 (McCoy and Mueller, 1992) is applied for the selective ^{13}C$^{\alpha}$ decoupling during t_1. All the pulsed field gradients are 1 ms with the following strengths: $G_1 = 4$ G/cm; $G_2 = 5.5$ G/cm; $G_3 = 9.3$ G/cm; $G_4 = 15.5$ G/cm; $G_5 = 22$ G/cm; $G_6 = 30.1$ G/cm. (C) Pulse sequence for the determination of the $^{1}J_{\mathrm{C'C}^{\alpha}}$ coupling by the 2D HN(CO-α/β-C′C$^{\alpha}$-*J*)-TROSY experiment. The delays employed are $\Delta = 1/(4J_{\mathrm{NH}})$; $\mathrm{T_a} = 1/(4J_{\mathrm{NC'}}) + \mathrm{T_b}/2 - \kappa * t_1/4$; $\mathrm{T'_a} = 1/(4J_{\mathrm{NC'}}) - \mathrm{T_b}/2 + \kappa * t_1/4$; $\mathrm{T_b} = 1/(4J_{\mathrm{C'C}^{\alpha}})$. Phase cycling for the in-phase spectrum: ϕ_1 = y, −y; ϕ_4 = 2(x), 2(−x); ϕ_5 = 4(x), 4(−x); ϕ_6 = 8(y), 8(−y); $\phi_{\mathrm{rec.}}$ = x, 2(−x), x. Phase cycling for the antiphase spectrum: ϕ_1 = x, −x; ϕ_6 = 8(x), 8(−x). All the pulsed field gradients are 1 ms with the following strengths: $G_1 = 4$ G/cm; $G_2 = 5.5$ G/cm; $G_3 = 12.3$ G/cm; $G_4 = 15.5$ G/cm; $G_5 = 22$ G/cm; $G_6 = 30.1$ G/cm. States-TPPI on ϕ_1. The constant κ can be adjusted between 0 and 1 for partial ^{15}N chemical shift evolution during polarisation transfer delays. The decoupling field is switched off prior to the application of the field gradient pulses (Kay, 1993).

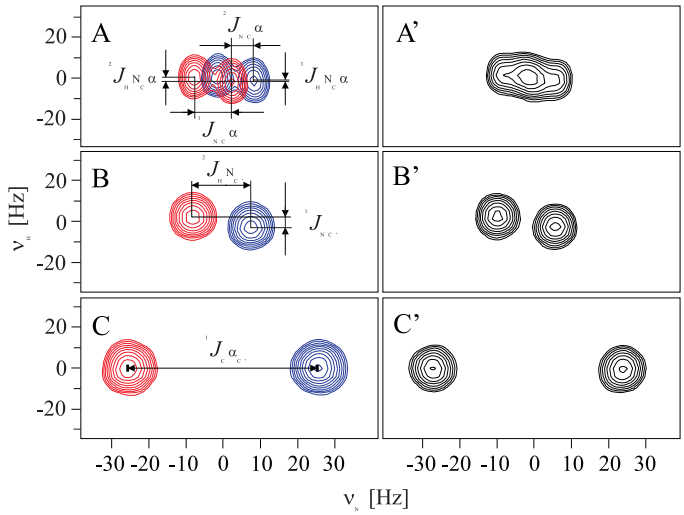

Figure 3. Expansions of (A) HN(CO-α/β-NC$^{\alpha}$-*J*), (B) HN(α/β-NC′-*J*), and (C) HN(CO-α/β-C′C$^{\alpha}$-*J*)-TROSY spectra, recorded from 1.0 mM U-(^{15}N, ^{13}C) ubiquitin, 90/10% H_2O/D_2O, 25 °C at 600 MHz ^{1}H frequency, $t_{1,\max}$ (t_2) = 222 (128) ms. Data were zero-filled to 4K × 4K data matrices and apodized with shifted squared sine-bell functions in both dimensions. Up- (blue) and downfield (red) multiplet components, processed to separate subspectra, are shown overlaid for Lys63. For reference, (A′) {^{13}C$^{\alpha}$}-^{15}N, (B′) {^{13}C′}-^{15}N, and (C′) HN(CO-C′C$^{\alpha}$-*J*)-TROSY spectra were acquired. The comparison of (A) with (A′) shows how the overlapping doublet of doublets is simplified by the spin-state selection.

residues (Delaglio et al., 1991). When the filter is tuned to a nominal 15 Hz, the intensity of the principal component over the minor component is at least 30-fold for ^{15}N-^{13}C′ couplings between 11.5–18.5 Hz, providing good filtering in the isotropic phase. In anisotropic phases maximal dipolar contributions of ± 2–3 Hz are expected when assuming at most 20–25 Hz dipolar contributions to the ^{15}N-^{1}H scalar couplings. Consequently, when there is simultaneously a large, i.e. 3 Hz, dipolar contribution and $^{1}J_{NC'}$ departs from the typical (14–16 Hz) scalar coupling, *J*-crosstalk due to the *J*-mismatch appears. In any case, the *J*-crosstalk artefacts arising from the *J*-mismatch, as well as from the unequal relaxation between the in-phase and antiphase magnetisations, can mostly be eliminated by scaling, that is, by taking an appropriate linear combination of the in- and antiphase spectra (Meissner et al., 1998b; Ottiger et al., 1998; Sørensen et al., 1999).

The HN(CO-α/β-C′C$^{\alpha}$-*J*)-TROSY experiment (Figure 2C) shares the same principle for the spin-state selection designed to suppress cross-correlation effects between dipole–dipole and CSA relaxation mechanisms (Goldman, 1984; Tjandra et al., 1996). The α- and β-spin-states of the corresponding ^{15}N-{^{13}C′} and ^{13}C′-{^{13}C$^{\alpha}$} doublets are inverted during the filter elements (Andersson et al., 1998b; Permi et al., 1999a, b). The tolerance for the *J*-mismatch of the filter used in the HN(CO-α/β-C′C$^{\alpha}$-*J*) is the same as in the HN(CO-α/β-NC$^{\alpha}$-*J*)-TROSY experiment (vide supra). In the in-phase experiment, for $\cos(\omega_N t_1)\cos(\pi\kappa J t_1)$ modulated data, the $4H_zN_xC'_y$ density operator is preserved by applying two 180° (^{13}C$^{\alpha}$) pulses at the midpoint of the T_b delays. In the antiphase experiment, for $\sin(\omega_N t_1)\sin(\pi\kappa J t_1)$ modulated data, the $4H_zN_xC'_y$ operator is converted into the $8H_zN_xC'_xC^{\alpha}_z$ coherence by applying an 180° (^{13}C$^{\alpha}$) pulse at the midpoint of $2{*}T_b$. The undesired dispersive contribution arising from the *J*-mismatch is purged by the 90° (^{13}C′) pulse following the filter element. During the subsequent evolution period $(1-\kappa){*}t_1$, the $^{1}J_{C'C^{\alpha}}$ coupling evolves simultaneously with the ^{15}N chemical shift. Improvement of the resolution and sensitivity can be achieved by partly incorporating the chemical shift evolution of ^{15}N ($\kappa{*}t_1$) into both ^{15}N-^{13}C′ out- and ^{13}C′-^{15}N back-transfer steps (Figure 2C). This accordion-style spectroscopy (Bodenhausen and Ernst, 1981) with a concomitant downscaling of the apparent splitting using the double semi-constant time (DS-CT) evolution is advantageous for larger proteins owing to their faster ^{15}N transverse relaxation. We find a good compromise between the sensitivity and precision when the coupling evolves for half of the time of the chemical shift evolution. Finally, since $^{1}J_{C'C^{\alpha}}$ is large and spin-state-selective filtering is used to remove the overlapping α- and β-states of a $^{13}C'_{i-1}$-$^{13}C^{\alpha}_{i-1}$ doublet,

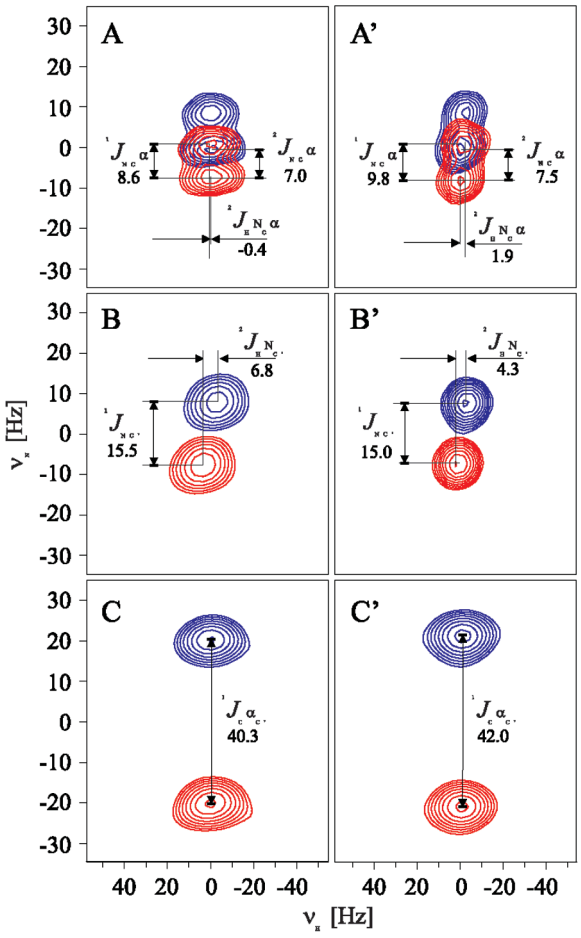

Figure 4. Expansions of (A) HN(CO-α/β-NC$^{\alpha}$-*J*), (B) HN(α/β-NC′-*J*), and (C) HN(CO-α/β-C′C$^{\alpha}$-*J*)-TROSY spectra, recorded from U-(^{15}N, ^{13}C) cNTnC (0.5 mM) in a dilute liquid crystal (left) and in water (2.0 mM) (right) at 30 °C, $t_{1,\max}$ (t_2) = 142 (128) ms. Shown for the major conformer of Asp87, the differences between the measured couplings (Hz) reveal the dipolar contribution for (A) the intraresidue $^1J_{NC^{\alpha}}$ and $^2J_{H^NC^{\alpha}}$, and interresidue $^2J_{NC^{\alpha}}$ (for this particular residue the dipolar contribution to the interresidue $^3J_{H^NC^{\alpha}}$ is below the measurement precision). (B) $^1J_{NC'}$ and $^2J_{H^NC'}$, and (C) $^1J_{C'C^{\alpha}}$ (scaled by 0.80). When using a perdeuterated sample, although not available for this study, improved resolution in the $^1H^N$ dimension will be available especially in the anisotropic phase, allowing more precise measurement of $^2(J+D)_{H^NC^{\alpha}}$, $^2(J+D)_{H^NC'}$, and $^3(J+D)_{H^NC^{\alpha}}$.

HN(CO-α/β-C′C$^{\alpha}$-*J*)-TROSY can easily be converted into a three-dimensional HNCO(α/β-C′C$^{\alpha}$-*J*)-TROSY experiment.

The sensitivity of the three experiments can be improved by converting the polarisation from the ^{15}N steady-state magnetisation to the N_x term to add to the $2H_zN_x$ coherence (Pervushin et al., 1998a; Salzmann et al., 1998; Yang et al., 1999), although cross

Table 1. Number of couplings measured from cTnC by α/β-*J*-TROSY experiments[a,b]

Coupling	Isotropic	Anisotropic[c]
$^1J_{H^NN}$	144 (117)	135 (108)
$^1J_{NC'}$	144 (128)	132 (112)
$^1J_{C'C^{\alpha}}$	142 (118)	125 (114)
$^1J_{NC^{\alpha}}$	135 (110)	108 (96)
$^2J_{H^NC'}$	144 (128)	132 (112)
$^2J_{H^NC^{\alpha}}$	138 (113)	112 (104)
$^2J_{NC^{\alpha}}$	135 (110)	108 (96)
$^3J_{H^NC^{\alpha}}$	138 (113)	112 (104)

[a]In parentheses are given the number of couplings in which measurement is not affected by cross peak overlap.
[b]$^1J_{H^NN}$ were measured using the generalized α/β-TROSY experiment (Andersson et al., 1998c).
[c]Dilute liquid crystal was composed of Pf1 particles, $D_{\|}^{HN} = 15$ Hz.

talk artefacts due to the undesirable ^{15}N-^{1}H multiplet component may need to be considered. The phase cycling of the three pulse sequences (Figure 2) can be revised as described (Pervushin et al., 1998a) to include ^{15}N steady-state magnetisation provided that the initial 90° (^{15}N) pulse followed by the dephasing gradient is removed, of course. Relaxation losses can be furthermore reduced by concatenating the ^{13}C′-^{15}N back-transfer step with the following ^{15}N-^{1}H INEPT (Pervushin et al., 1998b; Meissner et al., 1999) in the HN(CO-α/β-C′C$^{\alpha}$-*J*)- and HN(CO-α/β-NC$^{\alpha}$-*J*)-TROSY experiments, but we used the semi-constant time versions of the experiments (Figure 2) in which ^{15}N chemical shifts and ^{15}N-^{13}C$^{\alpha}$ coupling evolve during the ^{15}N-^{13}C′ polarisation transfer. The three experiments are compatible with various ways of water suppression. We prefer the water flip-back implementation to ensure that most of the water magnetisation is preserved along the positive z-axis throughout the pulse sequences and residual transverse magnetisation is effectively dephased by the pulsed field gradients (Piotto et al., 1992; Grzesiek and Bax, 1993b). Effects of preserving water magnetisation along the z-axis on signal intensity of a TROSY experiment have recently been discussed in detail (Rance et al., 1999).

Enhanced anisotropic tumbling of molecules in a dilute liquid crystal gives rise to readily observable residual dipolar couplings (Tjandra and Bax, 1997). The spin-state selective *J*-TROSY experiments record most of the dipolar couplings accessible to measurements from perdeuterated proteins in order

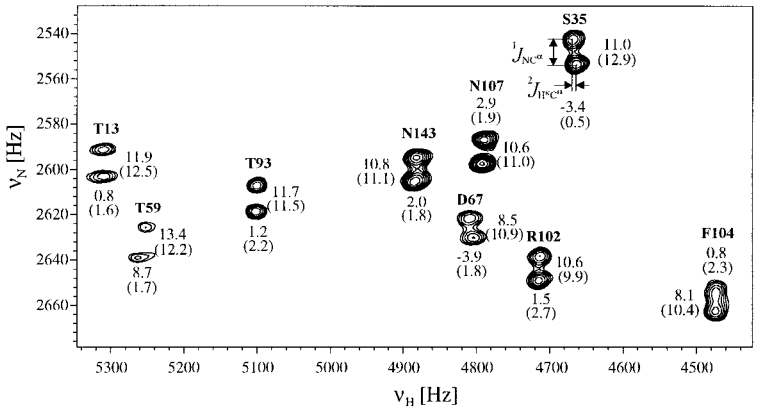

Figure 5. Expansion of HN(CO-α/β-NC$^{\alpha}$-*J*) subspectrum recorded from U-(^{15}N, ^{13}C) 18 kDa cTnC (0.5 mM) in a dilute liquid crystal at 40 °C, $t_{1,\max}$ (t_2) = 142 (128) ms. The spectrum processed for resolution enhancement contains in the in-phase multiplet components the intraresidue $^1(J+D)_{NC^{\alpha}}$ and $^2(J+D)_{H^NC^{\alpha}}$ couplings along the ^{15}N and ^{1}H dimensions, respectively. The corresponding scalar couplings shown in parentheses were measured from a reference spectrum recorded from cTnC dissolved in water.

to sample thoroughly polypeptide backbone orientation. Figure 4 illustrates how the dipolar contributions are measured from the α/β-*J*-TROSY spectra recorded from the regulatory domain of cardiac troponin C (cNTnC) dissolved in water and in a dilute liquid crystal composed of filamentous phage particles (Hansen et al., 1998). The interresidue $^1H^N$-$^{13}C^{\alpha}_{i-1}$ and ^{15}N-$^{13}C^{\alpha}_{i-1}$ couplings acquired with the HN(CO-α/β-NC$^{\alpha}$-*J*)-TROSY experiment (Figures 4A and A′) can be measured also if the intraresidue $^1H^N$-$^{13}C^{\alpha}$ and ^{15}N-$^{13}C^{\alpha}$ couplings are poorly resolved simply by apodizing for broadening. For the HN(α/β-NC′-*J*)-TROSY data (Figures 4B and B′), cross talk artefacts were suppressed by taking a linear combination, with the factor 0.92 estimated from the 1D traces, of the in- and antiphase spectra. The apparent C′C$^{\alpha}$ splittings in the HN(CO-α/β-C′C$^{\alpha}$-*J*)-TROSY spectra (Figures 4C and C′), acquired with DS-CT, correspond to $^1J_{C'C^{\alpha}}$ scaled down by a factor 0.80. To demonstrate the possibilities of the HN(CO-α/β-NC$^{\alpha}$-*J*)-TROSY experiment, in particular, in the measurement of the intraresidue $^1H^N$-$^{13}C^{\alpha}$ and ^{15}N-$^{13}C^{\alpha}$ couplings, which are certainly the most challenging, we recorded data of a 18 kDa cardiac troponin C (cTnC) dissolved in the dilute liquid crystal. The intraresidue in-phase spectrum reveals the dipolar contributions both to the $^1H^N$-$^{13}C^{\alpha}$ and ^{15}N-$^{13}C^{\alpha}$ couplings (Figure 5). The number of assigned couplings that we measured from the ^{15}N,^{13}C labeled cTnC sample using the α/β-*J*-TROSY experiments are listed in Table 1.

Conclusions

The combination of destructive relaxation interference, spin-state selection and perdeuteration allows the measurement of several, even comparatively small dipolar couplings. It is then possible to derive more precisely components of an alignment tensor to compute values corresponding to dipolar couplings from internuclear vectors (Clore et al., 1998a, b; Moltke and Grzesiek, 1999) defined by atomic coordinates to generate and refine structures, and make comparisons with X-ray structures or with known homologous structures. It is conceivable that the set of α/β-*J*-TROSY experiments will be useful in studies of SAR by NMR (Hajduk et al., 1996) to observe, in addition to amide chemical shift changes, also conformational changes induced by ligand binding. These novel methods further expand the possibilities of NMR in structural biology.

Acknowledgements

Cardiac troponin C is courtesy of Paul R. Rosevear. We thank Tia Sorsa and Kimmo Pääkkönen for the preparation of Pf1 and cNTnC. This work was supported by the Academy of Finland.

References

Andersson, P., Nordstrand, K., Sunnerhagen, M., Liepinsh, E., Turovskis, I. and Otting, G. (1998a) *J. Biomol. NMR*, **11**, 445–450.

Andersson, P., Weigelt, J. and Otting, G. (1998b) *J. Biomol. NMR*, **12**, 435–441.
Andersson, P., Annila, A. and Otting, G. (1998c) *J. Magn. Reson.*, **133**, 364–367.
Annila, A., Aitio, H., Thulin, E. and Drakenberg, T. (1999) *J. Biomol. NMR*, **14**, 223–230.
Bax, A., Ikura, M., Kay, L.E., Torchia, D.A. and Tschudin, R. (1990) *J. Magn. Reson.*, **86**, 304–318.
Bax, A. and Tjandra, N. (1997) *J. Biomol. NMR*, **10**, 289–292.
Bodenhausen, G. and Ruben, D. (1980) *Chem. Phys. Lett.*, **69**, 185–188.
Bodenhausen, G. and Ernst, R.R. (1981) *J. Magn. Reson.*, **45**, 367–373.
Bystrov, V.F. (1976) *Progr. NMR Spectrosc.*, **10**, 44–81.
Clore, G.M., Gronenborn, A.M. and Tjandra, N. (1998a) *J. Magn. Reson.*, **131**, 159–162.
Clore, G.M., Gronenborn, A.M. and Bax, A. (1998b) *J. Magn. Reson.*, **133**, 216–221.
Czisch, M. and Boelens, R. (1998) *J. Magn. Reson.*, **134**, 158–160.
Delaglio, F., Torchia, D.A. and Bax, A. (1991) *J. Biomol. NMR*, **1**, 439–446.
Fesik, S.W. (1993) *J. Biomol. NMR*, **3**, 261–269.
Goldman, M. (1984) *J. Magn. Reson.*, **60**, 437–452.
Griesinger, C., Sørensen, O.W. and Ernst, R.R. (1985) *J. Am. Chem. Soc.*, **107**, 6394–6396.
Griesinger, C., Sørensen, O.W. and Ernst, R.R. (1986) *J. Chem. Phys.*, **85**, 6837–6852.
Griesinger, C., Sørensen, O.W. and Ernst, R.R. (1987) *J. Magn. Reson.*, **75**, 474–492.
Grzesiek, S. and Bax, A. (1993a) *J. Biomol. NMR*, **3**, 185–204.
Grzesiek, S. and Bax, A. (1993b) *J. Am. Chem. Soc.*, **115**, 12593–12594.
Hajduk, P.J., Meadows, R.P. and Fesik, S.W. (1996) *Science*, **274**, 1531–1534.
Hansen, M.R., Mueller, L. and Pardi, A. (1998) *Nat. Struct. Biol.*, **12**, 1065–1074.
Kay, L.E. (1993) *J. Am. Chem. Soc.*, **115**, 2055–2056.
Logan, T.M., Olejniczak, E.T., Xu, R.X. and Fesik, S.W. (1993) *J. Biomol. NMR*, **3**, 225–231.
Marion, D., Ikura, M., Tschudin, R. and Bax, A. (1989) *J. Magn. Reson.*, **85**, 393–399.
McCoy, M. and Mueller, L. (1992) *J. Am. Chem. Soc.*, **114**, 2108–2112.
Meissner, A., Duus, J.Ø. and Sørensen, O.W. (1997a) *J. Biomol. NMR*, **10**, 89–94.
Meissner, A., Duus, J.Ø. and Sørensen, O.W. (1997b) *J. Magn. Reson.*, **128**, 92–97.
Meissner, A., Schulte-Herbrüggen, T., Briand, J. and Sørensen, O.W. (1998a) *Mol. Phys.*, **95**, 1137–1142.
Meissner, A., Schulte-Herbrüggen, T. and Sørensen, O.W. (1998b) *J. Am. Chem. Soc.*, **120**, 7989–7990.
Meissner, A. and Sørensen, O.W. (1999) *J. Magn. Reson.*, **139**, 439–442.
Moltke, S. and Grzesiek, S. (1999) *J. Biomol. NMR*, **15**, 77–82.
Ottiger, M., Delaglio, F. and Bax, A. (1998) *J. Magn. Reson.*, **131**, 373–378.
Permi, P., Heikkinen, S., Kilpeläinen, I. and Annila, A. (1999a) *J. Magn. Reson.*, **140**, 32–40.
Permi, P., Sorsa, T., Kilpeläinen, I. and Annila, A. (1999b) *J. Magn. Reson.*, **141**, 44–51.
Pervushin, K., Riek, R., Wider, G. and Wüthrich, K. (1997) *Proc. Natl. Acad. Sci. USA*, **94**, 12366–12371.
Pervushin, K., Wider, G. and Wüthrich, K. (1998a) *J. Biomol. NMR*, **12**, 345–348.
Pervushin, K., Ono, A., Fernandez, C., Szyperski, T., Kainosho, M. and Wüthrich, K. (1998b) *Proc. Natl. Acad. Sci. USA*, **95**, 14147–14151.
Pervushin, K., Riek, R., Wider, G. and Wüthrich, K. (1998c) *J. Am. Chem. Soc.*, **120**, 6394–6400.
Piotto, M., Sauder, V. and Sklenar, V.J. (1992) *J. Biomol. NMR*, **2**, 661–665.
Rance, M., Loria, J.P. and Palmer III, A.G. (1999) *J. Magn. Reson.*, **136**, 92–101.
Salzmann, M., Pervushin, K., Wider, G., Senn, H. and Wüthrich, K. (1998) *Proc. Natl. Acad. Sci. USA*, **95**, 13585–13590.
Salzmann, M., Wider, G., Pervushin, K., Senn, H. and Wüthrich, K. (1999) *J. Am. Chem. Soc.*, **121**, 844–848.
Shuker, S.B., Hajduk, P.J., Meadows, R.P. and Fesik, S.W. (1997) *Science*, **278**, 497–499.
Sørensen, M.D., Meissner, A. and Sørensen, O.W. (1999) *J. Magn. Reson.*, **137**, 237–242.
Tjandra, N. and Bax, A. (1997) *Science*, **278**, 1111–1114.
Tjandra, N., Szabo, A. and Bax, A. (1996) *J. Am. Chem. Soc.*, **118**, 6986–6991.
Wang, Y.-X., Marquardt, J.L., Wingfield, P., Stahl, S.J., Lee-Huang, S., Torchia, D. and Bax, A. (1998) *J. Am. Chem. Soc.*, **120**, 7385–7386.
Yang, D. and Kay, L.E. (1999) *J. Am. Chem. Soc.*, **121**, 2571–2575.